# Degradation and Relaxation Kinetics of Polystyrene−Clay Nanocomposite Prepared by Surface Initiated Polymerization

**Sergey Vyazovkin,*,† Ion Dranca,† Xiaowu Fan,† and Rigoberto Advincula†,‡**

*Department of Chemistry, University of Alabama at Birmingham, 901 South 14th Street, Birmingham, Alabama 35294, and Department of Chemistry, University of Houston, Houston, Texas 77204*

*Received: March 15, 2004; In Final Form: May 15, 2004*

Thermogravimetry and differential scanning calorimetry (DSC) have been used to study the thermal and thermo-oxidative degradation of polystyrene (PS) and PS−clay nanocomposite. An advanced isoconversional method has been applied for kinetic analysis. Introduction of the clay phase increases the activation energy and affects the total heat of degradation that suggests a change in the reaction mechanism. The obtained kinetic data permit comparative assessment of fire resistance of the studied materials. Relaxation kinetics have been measured by DSC and dynamic mechanical analysis. As compared to virgin PS, the clay nanocomposite shows the glass transition at a higher temperature and demonstrates markedly larger activation energy. This suggests that the clay phase lowers the molecular mobility of PS which is another factor contributing to the increased thermal stability of the nanocomposite.

## Introduction

Implanting layered silicates into polymers is known[1] to modify dramatically various physical properties including thermal stability and fire resistance.[2] A great deal of attention has been focused on the thermal behavior of polystyrene (PS)−clay nanocomposites[3−10] as studied by using cone calorimetry as well as standard thermal analysis methods such as thermogravimetric analysis (TGA), differential scanning calorimetry (DSC), and dynamic mechanical analysis (DMA). It has been found that compared to virgin PS the clay nanocomposites have a somewhat higher glass transition temperature[4,6] and mechanical modulus,[6,10] decompose at significantly greater temperatures,[4,7−9] and demonstrate a substantial decrease in the maximum heat release rate on combustion.[5,7−9]

It should be stressed that even when clay content is as little as 0.1%, the initial decomposition temperature is increased by 40 °C and the peak heat release rate is decreased by about 40% relative to virgin PS.[7] The mechanism of such remarkable effect is not yet well understood. The effect is most commonly rationalized in terms of the barrier model that suggests the enhanced fire resistant properties to arise due to a carbonaceous-silicate char that builds up on the surface of the polymer melt and provides the mass and heat transfer barrier.[5,9,11,12] It has also been suggested that the effect may be associated with radical trapping[8] by the structural iron in clays.

Although the thermal behavior of polymer−clay nanocomposites has been studied extensively, the kinetic aspects of degradation and relaxation remain practically unknown. The importance of reliable kinetic analysis cannot be overestimated as it may provide information on the energy barriers of the process as well as offer mechanistic clues. This paper is intended to initiate systematic kinetic studies of polymer nanocomposites and, therefore, to fill the presently existing void in the understanding of the thermal behavior of these exciting materials.

## Experimental Section

The PS−clay nanocomposite was prepared by intercalating a monocationic free radical initiator into montmorillonite clay and the subsequent solution surface-initiated polymerization (SIP), where the chain growth was initiated in situ from clay surfaces (Scheme 1). The montmorillonite clay (commercially Cloisite $Na^+$, cation exchange capacity 92 mequiv/100 g, specific surface area 750 $m^2/g$) we used was donated by Southern Clay Product Inc.. The initiator we synthesized was an azobisisobutyronitrile (AIBN)-analogue molecule with a quaternized amine group at one end. The intercalation process was realized by cation exchange reaction in which the cationic end of the initiator was ionically attached to the negatively charged clay surfaces. The synthesis of the initiator and the preparation of intercalated clays have been described in previous publications.[13,14] The subsequent SIP with the clay that had been intercalated by the initiator was performed in THF solvent with styrene as the monomer, resulting in a PS−clay nanocomposite by the in situ polymerization (Scheme 1).

The clay load was 0.5% that was evaluated as the mass of clay per the total mass of clay and styrene monomer. Details of the procedures of the SIP process and product isolation and analysis can be found in another publication.[13] This free radical SIP strategy can achieve exfoliated PS−clay nanocomposites with an even higher clay load of ∼1% by using the same monocationic initiator.[13] The molecular weight (∼90 000) and polydispersity (∼2.3) of the product were measured by size exclusion chromatography (SEC) using PS standards. The obtained material will be referred to as nPS90. For comparison purposes, we have used virgin radically polymerized PS (MW = 100 000) that was purchased from Alfa Aesar and used as received. The material will be referred to as PS100. According to our measurements, polydispersity of PS100 is 2.4. A few TGA runs have also been performed on an available small amount of PS that had been synthesized by using the AIBN

* To whom correspondence should be addressed. E-mail: vyazovkin@uab.edu.
† University of Alabama.
‡ University of Houston.

10.1021/jp048840d CCC: $27.50 
Published on Web 07/09/2004

**SCHEME 1**

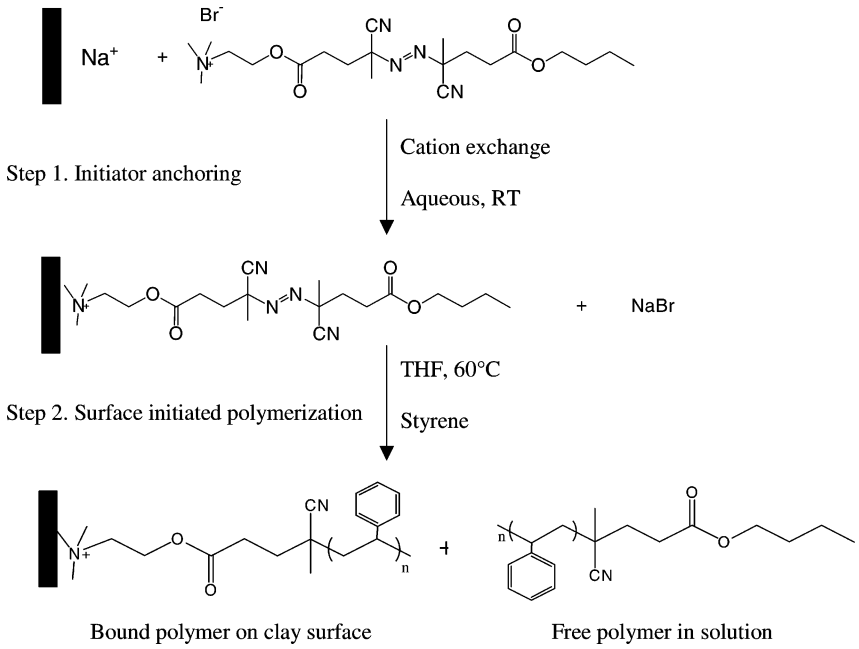


initiator. Because degradation of this material, denoted PS124 (MW = 124 000, polydispersity = 2.7), has been practically identical with that of PS100 (Figures 1 and 2), we have decided to use the latter which has been available to us in a large quantity and a form convenient for analyses. Another important reason for comparing nPS90 against PS100 is that their respective molecular weights and polydispersities are very close so that the effect of these factors on degradation and relaxation should be similar for both materials.

The degradation kinetics have been measured as the temperature-dependent mass loss by using a Mettler-Toledo TGA/SDTA851[e] module. Polymer samples of ∼5 mg have been placed in 40 $\mu$L Al pans and heated from 30 to 600 °C at the heating rates 2.5, 5.0, 7.5, 10.0, and 12.5 °C min$^{-1}$. Thermal and thermo-oxidative degradations have been respectively performed in the flowing atmosphere of $N_2$ and air at a flow rate of 70 mL min$^{-1}$. The buoyancy effect in TGA has been accounted for by performing empty pan runs and subtracting the resulting data from the subsequent sample mass loss data.

DSC measurements have been conducted by using a Mettler-Toledo DSC 822[e] module. For degradation studies, the conditions of DSC runs have been similar to those of TGA except that only one heating rate (10 °C min$^{-1}$) was used. The glass transition (relaxation) kinetics have been measured on 10 mg samples that have been first heated ∼40 °C above its glass transition temperature and held at this temperature for a short period to erase thermal history. The samples were then cooled to ∼40 °C below the glass transition temperature at rates from 5 to 25 °C min$^{-1}$. Immediately after completion of the cooling segment, the samples were heated at a rate whose absolute value is equal to the rate of preceding cooling as required by the kinetic method described further. Both DSC and TGA have been calibrated by using an Indium standard. To determine the clay content, three repetitive TGA runs under $N_2$ and air have been performed on ∼25 mg samples of nPS90 that have been heated in alumina pans up to 1000 °C. The amount of residue has been ∼1% in all runs. This amount should be related to the calcined clay content because the clay itself undergoes a small mass loss of about 3%.[14]

Dynamic mechanical analysis (DMA, Tritec 2000) has been performed to measure the relaxation kinetics and the mechanical modulus of the materials. DMA runs were carried out by using films and polymer impregnated cloth in the tension mode. For kinetic measurements, the samples were heated at 1 °C min$^{-1}$

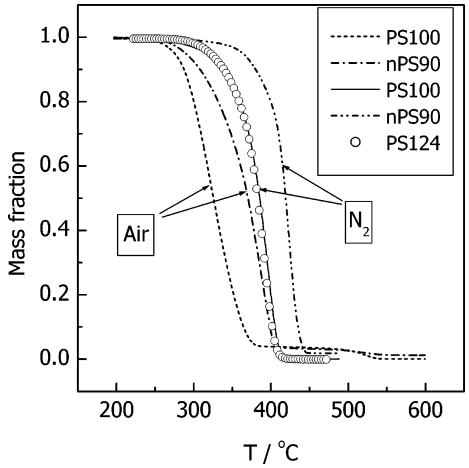


**Figure 1.** TGA curves for degradation of PS100, PS124, and nPS90 at heating rate 5 °C min$^{-1}$ in air and nitrogen.

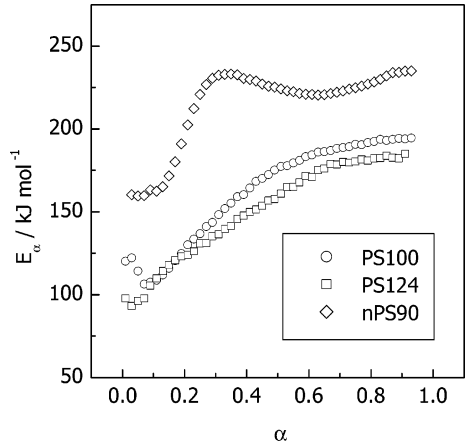


**Figure 2.** Dependence of the effective activation energy on the extent of conversion for the thermal degradation of PS100, PS124, and nPS90 in nitrogen.

at different frequencies ranging from 0.1 to 10 Hz. The modulus was measured at 0.4 Hz in an isothermal mode at 25 °C. The samples were of a rectangular shape 5 × 6 mm$^2$. The thickness of films was about 0.1 mm, and that of impregnated cloths, about 0.3 mm. The films were solvent cast (THF) on a glass surface. The cloth samples were produced by soaking cotton cloth into the polymer solution. After drying, the samples were annealed for 10 min in a furnace and slowly cooled to a room temperature. The annealing temperature was 130 °C for PS100 and 140 °C for nPS90.

**Kinetic Methods.** The overall rate of polymer degradation is commonly described by the following equation[15]

$$\frac{d\alpha}{dt} = A \exp\left(\frac{-E}{RT}\right) f(\alpha) \tag{1}$$

where α is the extent of polymer conversion, $t$ is the time, $T$ is the temperature, $R$ is the gas constant, $A$ is the pre-exponential factor, $E$ is the activation energy, and $f(\alpha)$ is the reaction model. Finding a proper way of kinetic analysis presents a certain challenge. Kinetic analysis is frequently reduced to fitting eq 1 to a data set obtained at a single heating rate. Computational flaws of the single heating rate analysis have been repeatedly stressed.[15,16] The recent publication[17] summarizing the results of the ICTAC Kinetics Project has recommended the use of multiple heating rate methods such as isoconversional methods.[15] Also, degradation of polymers tends to demonstrate complex kinetics[18] that cannot be described by only eq 1 throughout the whole temperature region.[19,20] To adequately represent the temperature dependence of degradation, one may use a model that involves several steps such as recombination, random scission, and end chain scission, each of which is represented by the respective eq 1.[21] However, simultaneously solving of three kinetic equations presents a considerable computational problem. A simpler alternative is to use a model-free isoconversional method. The method is based on the isoconversional principle that states that, at a constant extent of conversion, the reaction rate is only a function of the temperature:

$$\left[\frac{d\ln(d\alpha/dt)}{dT^{-1}}\right]_\alpha = -\frac{E_\alpha}{R} \tag{2}$$

(henceforth the subscript α indicates the values related to a given conversion). The isoconversional rates in eq 2 are determined as the rates to reach a given extent of conversion in several runs performed at different heating programs. While based on eq 1, the method assumes that $E_\alpha$ is constant only at a given extent of conversion and the narrow temperature region related to this conversion at different heating rates. In other words, the isoconversional methods describe the degradation kinetics by using multiples of eq 1, each of which is associated with a certain extent of conversion and has its own value of $E_\alpha$. The $E_\alpha$ values have a meaning of the effective activation energy. The resulting experimental dependence of $E_\alpha$ on α reflects changes of a limiting step[15,19,20,22,23] and represents adequately the temperature dependence of complex processes as proven by successful kinetics predictions[24,25] (vide infra, eq 5). Note that obtaining correct values of the effective activation energy is also important for simulation of polymer combustion.[26]

In this paper, we employ an advanced isoconversional method[27,28] in order to obtain reliable kinetic information on the thermal and thermoxidative degradation of PS−clay nanocomposite. The method was developed by Vyazovkin[27,28] and offers two major advantages over the frequently used methods of Flynn and Wall[29] and Ozawa.[30] The first advantage is that the method has been designed to treat the kinetics that occur under arbitrary variation in temperature, $T(t)$ which allows one to account for self-heating/cooling detectable by the thermal sensor of the instrument. For a series of $n$ experiments carried out under different temperature programs, $T_i(t)$, the activation energy is determined at any particular value of α by finding $E_\alpha$, which minimizes the function

$$\Phi(E_\alpha) = \sum_{i=1}^{n}\sum_{j\neq i}^{n} \frac{J[E_\alpha, T_i(t_\alpha)]}{J[E_\alpha, T_j(t_\alpha)]} \tag{3}$$

where

$$J[E_\alpha, T_i(t_\alpha)] \equiv \int_{t_\alpha-\Delta\alpha}^{t_\alpha} \exp\left[\frac{-E_\alpha}{RT_i(t)}\right] dt \tag{4}$$

The second advantage is associated with performing integration over small time segments (eq 4) that allows for eliminating a systematic error[28] occurring in the Flynn and Wall and Ozawa methods when $E_\alpha$ varies significantly with α. In eq 4, α is varied from Δα to 1 − Δα with a step $\Delta\alpha = m^{-1}$, where $m$ is the number of intervals chosen for analysis. The integral, $J$ in eq 4, is evaluated numerically by using the trapezoid rule. The minimization procedure is repeated for each value of α to find the dependence $E_\alpha$ on α.

Vyazovkin[24] proposed a model-free method that allows one to use nonisothermal data for predicting isothermal kinetics outside the experimental temperature region. By using kinetic data obtained at arbitrary temperature programs, one can estimate the time, $t_\alpha$, to reach a given conversion at an arbitrary isothermal temperature, $T_0$ by eq 5

$$t_\alpha = \frac{J[E_\alpha, T(t_\alpha)]}{\exp\left(\frac{-E_\alpha}{RT_0}\right)} \tag{5}$$

The $t_\alpha$ value is determined by substituting the experimentally determined values of $E_\alpha$ and $T_\alpha$ in eq 5. Repeating the procedure for different values of α results in obtaining an isothermal kinetic curve, α versus $t_\alpha$. Predictions made by eq 5 are called "model-free predictions" because they do not require knowledge of the reaction model, $f(\alpha)$. The reliability of such predictions has been demonstrated elsewhere.[24,25]

At ambient temperatures many polymers exist in the amorphous glassy state. This is an inherently nonequilibrium state that, on heating, relaxes toward the equilibrium liquid state. This particular type of relaxation is usually called the glass transition. The relaxation rate is described via a first-order kinetic equation[31]

$$\frac{d\xi}{dt} = -\frac{1}{\tau}(\xi - \xi_e) \tag{6}$$

where $\xi$ and $\xi_e$ are respectively the nonequilibrium and equilibrium values of an order parameter such as enthalpy or strain, and $\tau$ is the relaxation time. The temperature dependence of $\tau$ can be introduced via the Arrhenius equation

$$\tau = A \exp\left(\frac{E}{RT}\right) \tag{7}$$

The validity of eq 7 is supported by theoretical[32] and experimental[33] studies, which demonstrate that, below the glass transition temperature, $T_g$ the temperature dependence of $\tau$ changes its form from the WLF[34] to Arrhenius equation.

Although a complete treatment of glass transition kinetics is rather cumbersome,[35] the activation energy of the process can be evaluated in a very straightforward way.

DSC detects the glass transition process as a stepwise change in the heat capacity the midpoint of which is frequently used to determine the glass transition temperature. The apparent value of $T_g$ varies with the hating rate, $\beta$ that can be used for evaluating the activation energy of the glass transition. According to the method proposed by Moynihan et al.,[36,37] the activation energy can be determined by the following equation

$$E = -R\frac{\mathrm{d}\ln|\beta|}{\mathrm{d}T_g^{-1}} \tag{8}$$

The equation is applicable subject to the constraint that prior to heating the glassy material should be cooled from above to well below the glass transition region at a rate whose absolute value is equal to the rate of heating.

The glass−rubber transition (or so-called α-relaxation) can be revealed by DMA via the loss tangent (tan $\delta$) whose peak value is used to determine the transition temperature, $T_p$. The value of $T_p$ varies with the frequency, $f$. Due to the reciprocal relation between $f$ and $\tau$, eq 7 allows one to determine the activation energy of a transition from eq 9

$$E = -R\frac{\mathrm{d}\ln f}{\mathrm{d}T_p^{-1}} \tag{9}$$

The following section discusses the results of the application of the aforementioned methods to kinetic analysis of degradation and relaxation processes in the PS materials.

## Results and Discussion

**Degradation.** Figure 1 provides a comparison of the mass loss curves for degradation of virgin polymer and nanocomposite under nitrogen and air. PS100 degrades without forming any residue. Degradation of nPS90 leaves some residue in an amount of ∼1% that remains practically constant up to 1000 °C. Assuming PS has been completely volatilized, this number represents the amount of the clay phase in the nanocomposite. As seen in Figure 1, in both nitrogen and air the mass loss curves for nPS90 are found at markedly greater temperatures than the curves for PS100. The decomposition temperature increases by as much as 30−40 °C that is consistent with the results of other workers.[7−9] Given the small amount of the clay phase, this obviously represents a dramatic increase in thermal stability.

Figure 2 displays the results of the isoconversional kinetic analysis for the thermal degradation of PS100, PS124, and nPS90 in the atmosphere of nitrogen. For PS100 the effective activation energy increases from ∼100 to ∼200 kJ mol$^{-1}$ throughout degradation. Also observed was that degradation of the synthesized polymer PS124 is nearly identical with the degradation of the commercial polymer PS100, indicating that the latter is a valid reference material for nPS90. The variation in $E_\alpha$ indicates a change in a limiting step of the process. It has been suggested[38,39] that PS degradation is initiated at weak link sites inherent to the polymer itself such as head-to-head,[40] hydroperoxy,[38] and peroxy[39] structures. Once all of the weak link sites have given way to initiation, the mass loss of PS is controlled by the random scission process. In view of this mechanism, the increase in $E_\alpha$ most likely represents a shift of the limiting step from initiation at the weak links to random scission. Similar increases from smaller values of $E_\alpha$ have been observed for degradation of other polymers (PE, PP, and PMMA).[19,20] The values of $E_\alpha$ for nPS90 also show an increase with the extent of degradation that suggests a change in the rate limiting step. That latter occurs at the early stages of degradation ($\alpha < 0.25$) after which the effective activation energy practically levels off at 220−230 kJ mol$^{-1}$. The whole process of nPS90 degradation demonstrates a markedly larger effective activation energy as compared to that of PS100 degradation. According to our DSC data (Figure 3), the degradation of PS100 demonstrates a single endothermic peak. The nPS90 peak has a small shoulder at ∼400 °C and shows a smaller overall thermal effect. Based on a series of three measurements, the heats of degradation are −990 and −670 J g$^{-1}$ for PS100 and nPS 90, respectively.

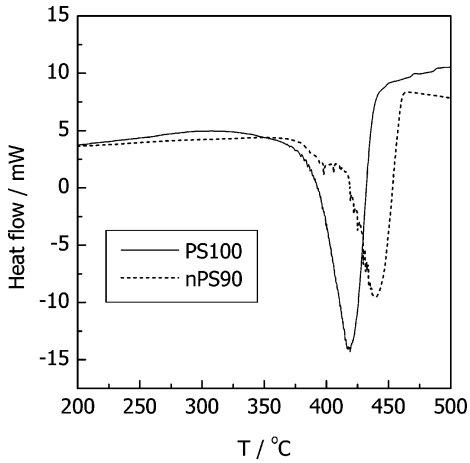


**Figure 3.** DSC curves for degradation of PS100 ($m$ = 4.84 mg) and nPS90 ($m$ = 5.16 mg) at heating rate 10 °C min$^{-1}$ in nitrogen.

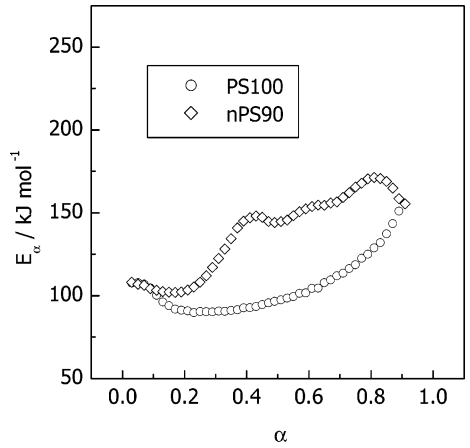


**Figure 4.** Dependence of the effective activation energy on the extent of conversion for the thermo-oxidative degradation of PS100 and nPS90 in air.

Figure 4 presents variations in $E_\alpha$ for thermo-oxidative degradation of PS100 and nPS90. For PS100, the initial stages of degradation occur with a lower activation energy of ∼90−100 kJ mol$^{-1}$ that later ($\alpha > 0.6$) rises to ∼150 kJ mol$^{-1}$. This behavior is consistent with the mechanism of thermo-oxidative degradation of PS that assumes[18,41] the initial formation of hydroperoxide radicals whose decomposition determines the degradation at early stages. At later stages and higher temperatures these radicals are no longer stable so that the degradation rate becomes controlled by unzipping. This mechanism is consistent with our DSC data (Figure 5) that show that initial stages of thermo-oxidative degradation are exothermic, whereas the later ones are endothermic. For nPS90, the initial degradation ($\alpha < 0.2$) demonstrates an activation energy similar to that for

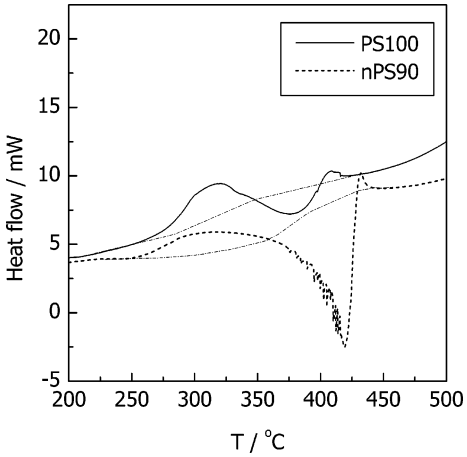


**Figure 5.** DSC curves for degradation of PS100 ($m$ = 4.88 mg) and nPS90 ($m$ = 5.38 mg) at heating rate 10 °C min$^{-1}$ in air. Dash−dot lines show conditional baselines.

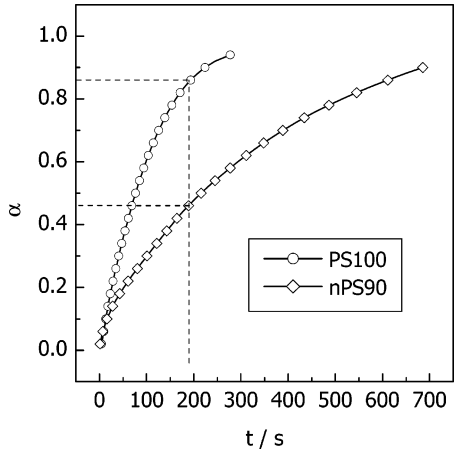


**Figure 6.** Predicted kinetic curves for the thermo-oxidative degradation of PS100 and nPS90 at temperature 380 °C.

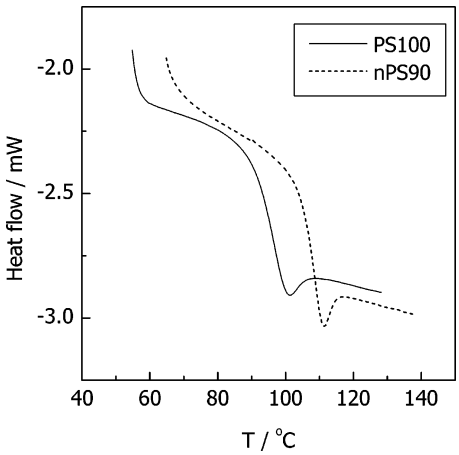


**Figure 7.** DSC curves for the glass transition at 10 °C min$^{-1}$.

degradation of PS100 that appears to suggest that the rate of the early degradation stages of both materials is limited by decomposition of hydroperoxide radicals. At $\alpha > 0.2$, the effective activation energy quickly rises to 150−170 kJ mol$^{-1}$ which is markedly larger than the activation energy for degradation of PS100 at similar extents of conversion. Although the size of the exotherms appears comparable (∼140 J g$^{-1}$ for nPS90 and ∼160 J g$^{-1}$ for PS100) for both materials, the endothermic effect in nPS90 is noticeably larger than that in PS100 (Figure 5). The values of degradation heat are about −100 J g$^{-1}$ for PS100 and −300 J g$^{-1}$ for nPS90. Obviously, the exact values are to some extent dependent on the choice of the baseline that is not a straightforward procedure in the case of overlapping processes as those observed in Figure 5.

Putting the above results together, we can conclude that the introduction of the clay phase into PS causes a considerable increase in the effective activation energy of degradation. The enhanced thermal stability of the PS−clay nanocomposites is likely to be associated with this increase. It does not seem that this result can be easily rationalized in terms of the barrier model, which suggests that the degradation rate of a polymer−clay nanocomposite should be limited by diffusion of gaseous decomposition products through the surface barrier of the silicate char. However, diffusion of gases in liquids and solids, including polymers, tends to have a low activation energy of about 40−50 kJ mol$^{-1}$.[42] Also the presence of the surface barrier cannot affect the total value of the heat of degradation. Nevertheless, the degradation of the nanocomposite in nitrogen demonstrates a 30% smaller endothermic effect than that for virgin PS. In air, the endothermic effect for nPS90 is about three times larger than the respective effects observed for PS100. These facts suggest that introduction of the clay phase in PS is likely to change the concentration distribution of degradation products and/or maybe cause the formation of some new products of degradation. This suggestion appears to correlate with the results of cone calorimetry experiments[5,7,9] which indicate that the clay enhanced PS composites tend to burn with releasing a significantly smaller amount of the total heat. This may be because the concentration distribution of degradation products changes toward the formation of less combustible products. Although the barrier model makes sense from both an experimental[9,11] and a theoretical standpoint,[12] the barrier formation does not seem to be the only reason that contributes to the enhanced thermal and fire stability of polymer−clay nanocomposites. The chemical effect of clay and ammonium moieties on the degradation mechanism appears to be equally important in enhancing these properties.

The obtained kinetic information on thermo-oxidative degradation of PS100 and nPS90 can be used for estimating the potential fire resistance of these materials. According to the cone calorimetry measurements[7] performed at a heat flux of 35 kW m$^{-2}$, virgin PS loses 86% of its mass for 190 s. By iteratively using eq 5, we find that for PS100 $\alpha = 0.86$ is reached for 190 s at $T_0$ = 380 °C (Figure 6). At this temperature the predicted mass loss for nPS90 at 190s is ∼46% that compares well with the values 53% and 54% measured experimentally[7] for some of the nanocomposites. This indicates that the obtained kinetic data are relevant to the combustion conditions. It should also be noted that the value $T_0$ = 380 °C is somewhat above the so-called flash ignition temperature that, according to ASTM D1929, is defined as the lowest initial temperature of air passing around the specimen, at which a sufficient amount of combustible gas is evolved to be ignited. For PS, the measured values of the flash ignition temperature are usually found in the region 345−360 °C.[43] Therefore, by using eq 5 for predicting the degradation kinetics at the flash ignition temperature, one can obtain comparative estimates for the potential fire resistance of polymeric materials.

**Relaxation.** DSC runs for both materials produced typical glass transition steps (Figure 7), the midpoint of which has been used as an estimate of the $T_g$ value. It is observed that in nPS90 the glass transition occurs at about 10 °C greater temperature than in PS100. The values of $T_g$ have been determined at 10 heating rates (2 times at each heating rate). Figure 8 displays

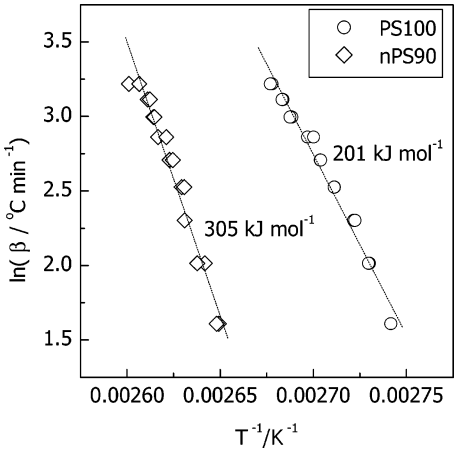


**Figure 8.** Evaluation of the activation energies for the glass transition by eq 8. Numbers by the linear segments show the respective values of *E*.

the resulting dependencies of $\ln\beta$ vs $T_g^{-1}$. The plots are nonlinear so that the activation energy decreases with temperature. This is consistent with the prediction of the WLF equation[34] that the effective activation energy for viscoelastic relaxation should decrease with increasing temperature as follows[44]

$$E = 2.303R\frac{c_1c_2T^2}{(c_2 + T - T_g)^2} \tag{10}$$

where $c_1$ and $c_2$ are the constants. The slopes of the $\ln\beta$ vs $T_g^{-1}$ plots yield averaged values of the effective activation energy for PS100 and nPS90 that, respectively, are 201 and 305 kJ mol$^{-1}$. The use of the isoconversional method allows one to determine a variation of *E* with the extent conversion from the glassy to rubbery state, α. This conversion can be evaluated from DSC data (Figure 7) as the normalized heat capacity[45] as follows

$$C_p^N = \frac{(C_p - C_{pg})|_T}{(C_{pe} - C_{pg})|_T} \equiv \alpha \tag{11}$$

where $C_p$ is the observed heat capacity, and $C_{pg}$ and $C_{pe}$ are, respectively, the glassy and equilibrium (liquid) heat capacity. Because the values of $C_{pg}$ and $C_{pe}$ are temperature dependent, they must be extrapolated into the glass transition region. According to Hodge,[45] the $C_p^N$ value provides a precise approximation to the temperature derivative of the fictive temperature. The application of the isoconversional method to the resulting α vs *T* data obtained at different heating rates yields the $E_\alpha$ dependencies shown in Figure 9. The activation energies decrease from 280 to 140 kJ mol$^{-1}$ for PS and from 350 to 160 for kJ mol$^{-1}$ for nPS90. The decrease is associated with decreasing the density of the polymers with increasing temperature. As the packing becomes looser, the chain segments gain more free volume and start to relax more independently that relieves energetic constrains. It should be stressed, however, that the respective activation energies for the glass transition in nPS90 are markedly greater than in PS100 throughout the glass transition region.

The initial set of DMA runs has been performed on solvent cast films. Unfortunately, the films have been found to quickly lose their elasticity as the materials undergo the glass−rubber transition. As a result, the loss tangent was increasing dramatically without showing regular peaks (Figure 10). However, the film runs have been used to measure the mechanical modulus

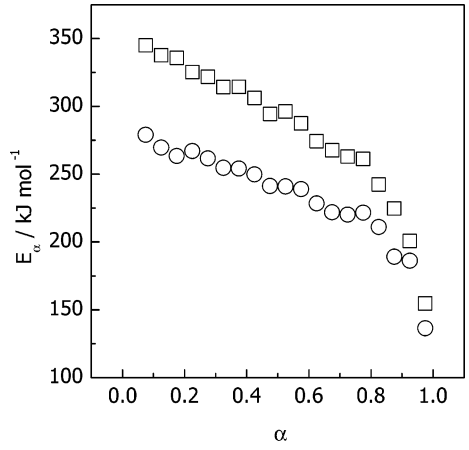


**Figure 9.** Activation energy as a function of the degree of conversion from the glassy to rubbery state.

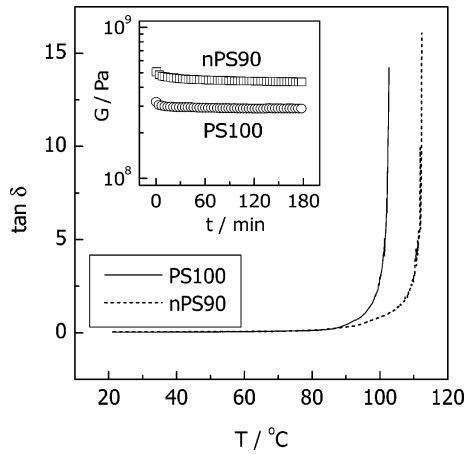


**Figure 10.** DMA runs on films at the frequency 1.0 Hz. Inset shows an isothermal run at 25 °C.

of the materials. Nonisothermal runs have shown that both materials have the modulus of about $10^8$ Pa. The values have been scattered, although for nPS90 the modulus values have been larger than those for PS100. We have found that isothermal runs provide more reproducible values. Typical results of the runs are shown in Figure 10. According to the isothermal data, nPS90 has an ∼1.5 larger modulus than that for PS100.

To be able to follow the glass−rubber transition throughout the whole process, we have performed a series of runs on polymer impregnated cloth samples. The use of a cloth[46] or braid[47] support provides a good practical solution to the problem of measuring transitions in low modulus samples. Before using, the cloth was tested in DMA and showed no events that might obscure the relaxation behavior of the polymers in the temperature region of interest, i.e., 20−150 °C. Figure 11 displays typical data of the cloth runs. Note that these runs yield global moduli that cannot be related to the respective values for unsupported PS100 and nPS90 (Figure 10) because the precise dimensional sizes of the polymer in the cloth samples cannot be determined. The temperatures of the peaks, $T_p$, have been used as the glass−rubber transition temperatures. It is seen that in nPS90 the transition occurs at temperatures ∼10 °C greater than those in PS100. The result is obviously consistent with our DSC measurements of the glass transition (Figure 7). The values of $T_p$ have been determined at five different frequencies, and the plots of ln*f* against $T_p^{-1}$ have been constructed (Figure 12). For PS100 the plot is nonlinear, although its higher temperature portion can be well approximated by a straight line that yields the activation energy 360 kJ mol$^{-1}$. For nPS90, the

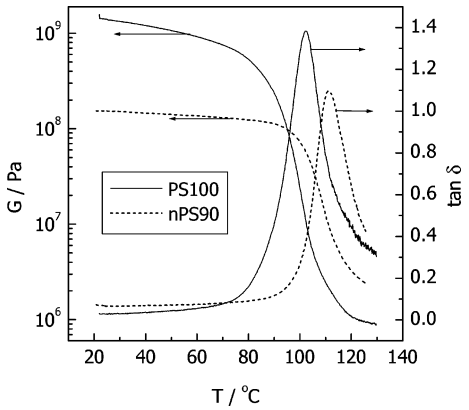


**Figure 11.** DMA runs on impregnated cloth samples at 0.5 Hz.

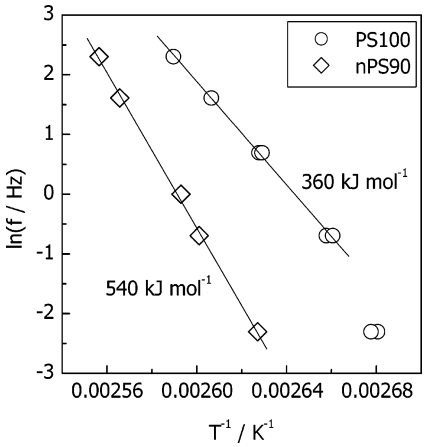


**Figure 12.** Evaluation of the activation energies for the glass−rubber transition by eq 9. Numbers by the straight lines show the respective values of *E*.

plot does not show any noticeable nonlinearity. The respective activation energy is 540 kJ mol$^{-1}$. Although the values derived from DMA runs are larger than the respective values obtained from DSC experiments, both methods clearly suggest that the glass transition in nPS90 has a significantly larger activation energy than that in PS100. It should also be noted that DMA as well as DSC derived values fall within the large interval, 160−900 kJ mol$^{-1}$ reported in the literature.[45,48−52]

Our relaxation data clearly indicate that the long chain molecular motion in the PS−clay nanocomposite encounters a markedly larger energy barrier than it does in virgin PS. That is at the same temperature the nanocomposite should have lower molecular mobility than the virgin polymer. Because the molecular mobility is the major factor that contributes to the transport of reactive species (e.g., oxygen and/or radicals) within the polymer, the nanocomposite is likely to have lower reactivity and, therefore, greater chemical and thermal stability than virgin PS.

Although the above conclusion is based on the lower temperature experiments, it is not impossible that the reduced chain mobility may also contribute to the increased thermal stability observed for the nanocomposite at the higher temperatures relevant to degradation. Figure 9 suggests that the activation energy for relaxation of nPS90 is greater than that of PS100 throughout the whole transition region. This tendency is likely to continue in the liquid state of the materials. For instance, it has been reported that the activation energies of the viscous flow are markedly larger for poly($\epsilon$-caprolactone)/clay[53] and polypropylene/clay[54] nanocomposites than for the respective virgin polymers. Regardless of the increase in the activation energy, a significant increase in viscosity appears to be commonly observed for various polymer−clay nanocomposites.[53−56] An increase in viscosity has a major impact on the kinetics of chemical reactions that occur in viscous reaction media,[57] because the effective characteristic time of a process, $t_{ef}$, is generally the sum of the characteristic time of a chemical act, $t_r$, and the characteristic time for reactants to diffuse in a viscous medium, $\tau$:[58]

$$t_{ef} = t_r + \tau \tag{12}$$

Because diffusion occurs as a succession of molecular jumps between the neighboring equilibrium positions, the characteristic time of the jump can be approximated by the relaxation time, which according to Debye[59] is

$$\tau = \frac{4\pi a^3 \eta}{kT} \tag{13}$$

where $\eta$ is the viscosity of the medium, $a$ is the molecular radius, and $k_B$ is Boltzmann's constant. With regard of eqs 12 and 13, it is obvious that an increase in viscosity slows down the overall process by increasing its effective characteristic time. Therefore, the reduced chain mobility can be one of the factors that delay degradation in polymer−clay composites.

## Conclusions

The kinetic analysis demonstrates that the processes of degradation and relaxation have noticeably larger activation energies in the clay composite than in virgin PS. The larger energy barrier for the glass transition indicates lowering the molecular mobility and, therefore, increasing chemical and physical stability. For degradation, the increase in the activation energy also means an increase in stability due to retarding the process. In addition it hints at a possible change in the mechanistic pathway that is supported by another important finding of our work that the clay phase in PS affects markedly the total heat of degradation. This fact points to a possible change in the concentration distribution of degradation products, the measurement of which will be a topic of our further work.

**Acknowledgment.** Thanks are due to Mettler-Toledo, Inc. for donation of the TGA instrument used in this work. Partial support for this work from the Army Research Office under Grant DAAD19-02-1-0190 is gratefully acknowledged.

## References and Notes

(1) Alexandre, M.; Dubois, P. *Mater. Sci. Eng., R* **2000**, *28*, 1.
(2) Porter, D.; E. Metcalfe, E.; Thomas, M. J. K. *Fire Mater.* **2000**, *24*, 45.
(3) Vaia, R. A.; Ishii, H.; Giannelis, E. P. *Chem. Mater.* **1993**, *5*, 1694.
(4) Noh, M. W.; Lee, S. C. *Polym. Bull.* **1999**, *42*, 619.
(5) Gilman, J. W.; Jackson, C. L.; Morgan, A. B.; Harris, P.; Manias, E.; Giannelis, E. P.; Wuthenow, M.; Hilton, D.; Phillips, S. H. *Chem. Mater.* **2000**, *12*, 1866.
(6) Okamoto, M.; Morita, S.; Taguchi, H.; Kim, Y. H.; Kotaka, T.; Tateyama, H. *Polymer* **2000**, *41*, 3887.
(7) Zhu, J.; Wilkie, C. A. *Polym. Int.* **2000**, *49*, 1158.
(8) Zhu, J.; Uhl, F. M.; Morgan, A. B.; Wilkie, C. A. *Chem. Mater.* **2001**, *13*, 4649.
(9) Morgan, A. B.; Harris, R. H.; Kashiwagi, T.; Chyall, L. J.; Gilman, J. W. *Fire Mater.* **2002**, *26*, 247.
(10) Wang, D.; Zhu, J.; Yao, Q.; Wilkie, C. A. *Chem. Mater.* **2002**, *14*, 3837.
(11) Wang, J.; Du, J.; Zhu, J.; Wilkie, C. A. *Polym. Degrad. Stab.* **2002**, *77*, 249.
(12) Lewin, M. *Fire Mater.* **2003**, *27*, 1.
(13) Fan, X.; Xia, C.; Fulghum, T.; Park, M.-K.; Locklin, J.; Advincula, R. C. *Langmuir* **2003**, *19*, 916.
(14) Fan, X.; Xia, C.; Advincula, R. C. *Colloids Surf., A* **2003**, *219*, 75.

(15) Flynn, J. H. In *Encyclopedia of Polymer Science and Engineering*; Mark, H. F., Bikales, N. M., Overberger, C. V., Kroschwitz, J. I., Eds.; J. Wiley & Sons: New York, 1989; Suppl. Vol., p 690.
(16) Vyazovkin, S.; Sbirrazzuoli, N. *Macromol. Chem. Phys.* **1999**, *200*, 2294.
(17) Brown, M. E.; Maciejewski, M.; Vyazovkin, S.; Nomen, R.; Sempere, J.; Burnham, A.; Opfermann, J.; Strey, R.; Anderson, H. L.; Kemmler, A.; Keuleers, R.; J. Janssens, J.; Desseyn, H. O.; Li, C.-R.; Tang, T. B.; Roduit, B.; Malek, J.; Mitsuhashi, T. *Thermochim. Acta* **2000**, *355*, 125.
(18) Flynn, J. H. In *Handbook of Thermal Analysis and Calorimetry*; Cheng, S. Z. D., Ed.; Elsevier: 2002; Vol. 3 p 587.
(19) Peterson, J. D.; Vyazovkin, S.; Wight, C. A. *J. Phys. Chem. B* **1999**, *103*, 8087.
(20) Peterson, J. D.; Vyazovkin, S.; Wight, C. A. *Macromol. Chem. Phys*. **2001**, *202*, 775.
(21) Kodera, Y.; McCoy, B. *Energy Fuels* **2002**, *16*, 119.
(22) Vyazovkin, S.; Sbirrazzuoli, N. *Macromolecules* **1996**, *29*, 1867.
(23) Vyazovkin, S.; Sbirrazzuoli, N. *J. Phys. Chem. B* **2003**, *107*, 882.
(24) Vyazovkin, S. *Int. J. Chem. Kinet.* **1996**, *28*, 95.
(25) Vyazovkin, S.; Wight, C. A. *Thermochim. Acta* **1999**, *340/341*, 53.
(26) Lyon, R. E. *Fire Mater.* **2000**, *24*, 179.
(27) Vyazovkin, S. *J. Comput. Chem.* **1997**, *18*, 393.
(28) Vyazovkin, S. *J. Comput. Chem.* **2001**, *22*, 178.
(29) Flynn, H.; Wall, L. A. *J. Res. Natl. Bur. Stand., Sect. A* **1966**, *70*, 487.
(30) Ozawa, T. *Bull. Chem. Soc. Jpn.* **1965**, *38*, 1881.
(31) Strobl, G. *The Physics of Polymers*, 2nd ed.; Springer: Berlin, 1997.
(32) Di Marzio, E. A.; Yang, A. J. M. *J. Res. Natl. Inst. Stand. Technol.* **1997**, *102*, 135.
(33) O'Connell, P. A.; McKenna, G. B. *J. Chem. Phys.* **1999**, *110*, 11054.
(34) Williams, M. L.; Landel, R. F.; Ferry, J. D. *J. Am. Chem. Soc*. **1955**, 77, 3701
(35) McKenna, G. B.; Simon, S. L. In *Handbook of Thermal Analysis and Calorimetry*; S. Z. D., Cheng, Ed.; Elsevier Science: 2002; Vol. 3, p 49.
(36) Moynihan, C. T.; Eastel, A. J.; Wilder, J. *J. Phys. Chem*. **1974**, *78*, 2673.
(37) Moynihan, C. T.; Lee, S.-K.; Tatsumisago, M.; Minami, T. *Thermochim. Acta* **1996**, *280*/*281*, 153.
(38) Madorsky, S. L. *Thermal Degradation of Organic Polymers*; Interscience Publishers: New York, 1964.
(39) Grassie, N.; Scott, G. *Polymer Degradation and Stabilisation;* Cambridge University Press: Cambridge, 1985.
(40) Howell, B. A.; Cui, Y.; Priddy, D. B. *Thermochim. Acta* **2003**, *396*, 167.
(41) Celina, M.; Ottesen, D. K.; Gillen, K. T.; Clough, R. L. *Polym. Degrad. Stab.* **1997**, *58*, 15.
(42) Jost, W. *Diffusion in solids, liquids, gases*; Academic Press: New York, 1960.
(43) Hilado, C. J. *Flammability Handbook for Plastics*, 5th ed.; CRC Press: New York, 1998.
(44) Ferry, J. D. *Viscoelastic Properties of Polymers*, 3rd ed.; J. Wiley: New York, 1980.
(45) Hodge, I. M. *J. Non-Cryst. Solids* **1994**, *169*, 211.
(46) Lee, C. Y. C.; Goldfarb, I. *J. Polym. Eng. Sci*. **1981**, *21*, 390.
(47) Gillham, J. K.; Enns, J. B. *Trends Polym. Sci*. **1994**, *2*, 406.
(48) McCrum, N. G.; Read, B. E.; Williams, G. *Anelastic and Dielectric Effects in Polymeric Solids*, Dover: New York, 1991.
(49) Boller, A.; Okazaki, I.; Wunderlich, B. *Thermochim. Acta* **1996**, *284*, 1.
(50) Gao, H.; Harmon, J. P. *Thermochim. Acta* **1996**, *284*, 85.
(51) Schawe, J. E. K. *J. Polym. Sci. B* **1998**, *36*, 2165.
(52) Simon, S. L.; Sobieski, J. W.; Plazek, D. J. *Polymer* **2001**, *42*, 2555.
(53) Kwak, S. Y.; Kwang, S. O. *Macromol. Mater. Eng.* **2003**, *288*, 503.
(54) Gu, S. Y.; Ren, J.; Wang, Q. F. *J. Appl. Polym. Sci*. **2004**, *91*, 2427.
(55) Galgali, G.; Ramesh, C.; Lele, A. *Macromolecules* **2001**, *34*, 825.
(56) Mitchell, C. A.; Krishnamoorti, R. *J. Polym. Sci., Part B: Polym. Phys.* **2002**, *40*, 1434.
(57) Vyazovkin, S.; Sbirrazzuoli, N. *Macromol. Chem. Phys.* **2000**, *201*, 199.
(58) Frank-Kamenetskii, D. A. *Diffusion and Heat Transfer in Chemical Kinetics*, 2nd ed.; Plenum Press: New York, London, 1969.
(59) Debye, P. *Polar Molecules*; The Chem. Catalog Co.: New York, 1929.